

# On the Relationship between FAPAR and NDVI

R. B. Myneni<sup>\*,†</sup> and D. L. Williams<sup>\*</sup>

*The influence of pixel heterogeneity, background, atmospheric and bidirectional effects on the relationship between fraction of photosynthetically active radiation absorbed by the photosynthesizing tissue in a canopy (FAPAR) and normalized difference vegetation index (NDVI) is investigated using a three-dimensional model of radiation transfer. Top of the canopy (TOC) NDVI and FAPAR increase with ground cover and plant leaf area. Their functional response to leaf orientation, solar zenith angle and atmospheric optical depth is similar. For instance, planophile canopies (mostly horizontal leaves) have a higher FAPAR and TOC NDVI than erectophile canopies (mostly erect leaves). However, FAPAR and TOC NDVI respond differently to other parameters such as soil reflectance and leaf optical properties. For example, an increase in soil reflectance increases FAPAR but decreases TOC NDVI. Atmospheric and bidirectional effects confound the interpretation of top of the atmosphere (TOA) NDVI. The transmissivity of NDVI, defined as the ratio TOA/TOC NDVI, decreases with increasing atmospheric turbidity and solar zenith angle. Sensing about the nadir directions under clear sky conditions and moderate solar incidence angles can result in transmissivities as high as 0.8. There are sufficient causal grounds for relating FAPAR to NDVI. The relationship is independent of pixel heterogeneity, parameterized here with ground cover, plant leaf area, and variations in leaf orientation and optical properties. On the other hand, the relationship is sensitive to background, atmospheric, and bidirectional effects. A simple linear model relating FAPAR to TOC NDVI is proposed, and its validity is discussed.*

## INTRODUCTION

The productivity of a vegetated surface is related, among other factors, to the fraction of incident photosynthetically active radiation (0.4–0.7  $\mu\text{m}$ ) absorbed by the photosynthesizing tissue in a canopy (FAPAR). An accurate specification of FAPAR is an important detail in large-scale productivity and carbon budget models (Prince, 1991). Ground cover and leaf area are perhaps the two most significant variables determining canopy PAR absorption. FAPAR (or its surrogate) can be vicariously determined from remote observations of surface spectral reflectance on the premise that surface structural and optical properties govern both these processes (Tucker, 1979).

There is substantial empirical evidence to suggest that FAPAR is related to top of the canopy spectral vegetation indices (Daughtry et al., 1983; Asrar et al., 1984; Hatfield et al., 1984; Gallo et al., 1985; Wiegand et al., 1991, 1992; Hall et al., 1992a,b; among others). This has also been demonstrated quasitheoretically using radiative transfer models of varying degree of detail (Sellers, 1985; Choudhury, 1987; Baret and Guyot, 1991; Asrar et al., 1992; Goward and Huemmrich, 1992; Myneni et al., 1992; among others). While this body of evidence is impressive, there are at least four issues that need to be addressed before this relationship can be used to convert satellite data of spectral reflectances to surface FAPAR values.

Pixel heterogeneity, background, atmospheric, and bidirectional effects are some of the most confounding problems in the analysis of satellite observations for surface information extraction. Pixel heterogeneity may be broadly defined to include spatial distribution of leaf area, fractional ground cover, and variations in leaf orientation and optical properties. The spatial distribution of radiance field and associated processes is affected by pixel heterogeneity. A quantitative analysis of pixel heterogeneity requires three-dimensional models of the physical problem because the lateral divergences are

<sup>\*</sup>Biospheric Sciences Branch, NASA Goddard Space Flight Center, Greenbelt

<sup>†</sup>University of Maryland Resident Associate

Address correspondence to Ranga B. Myneni, Biospheric Sciences Br., Code 923, NASA/GSFC, Greenbelt, MD 20771.

Received 25 February 1993; revised 20 April 1994.

nonzero  $[(\partial/\partial x) \text{ and } (\partial/\partial y) \neq 0]$  (Asrar et al., 1992). Diagnostic variables of surface state and processes that are independent of pixel heterogeneity are also scale-invariant, as we shall see later in this discussion.

Remote observations over a vegetated surface invariably contain contributions from the background soil and/or litter. When vegetation parameters such as FAPAR are of interest, background effects must be corrected. Moreover, the bidirectional reflectance distribution function of a vegetated surface is anisotropic and depends on the solar angles (Deering, 1989). Structurally rough surfaces like vegetation and soils are strong backscatterers while the atmosphere is predominantly a forward scatterer. Off-nadir satellite measurements gathered at different solar incidences (viz., AVHRR data) must be corrected for these bidirectional effects to assure uniformity in geometry before further analysis. Finally, the atmosphere introduces a positive (negative) effect at blue and red (near-infrared) wavelengths, that is, top of the atmosphere radiance is greater (lesser) than top of the surface radiance (Kaufman, 1989). Thus, even nadir measurements gathered at similar solar incidences must be corrected for atmospheric effects, and the single most important variable required for this correction is the atmospheric optical depth.

The objective of this article is to address the influence of pixel heterogeneity, background, atmospheric, and bidirectional effects on the relationship between FAPAR and the spectral vegetation index, normalized difference vegetation index (NDVI). This is accomplished by utilizing a three-dimensional model of radiation transfer in an atmosphere/vegetated-surface system (Myneni and Asrar, 1993). Theoretical and numerical considerations are highlighted in the next sections, followed by a discussion on the dynamics of NDVI and FAPAR, and the relation between the two. A simple linear model for this relationship is proposed and discussed.

## THEORETICAL CONSIDERATIONS

The physical problem can be described as follows. Consider a vegetated surface of indeterminate ground cover (partial or complete). We are interested in the angular distribution of the radiance field at the top of the vegetation canopy and the atmosphere, in the wavelength interval 0.4–2.25  $\mu\text{m}$ . Additionally, the fraction of incident radiation absorbed by the canopy in the interval 0.4–0.7  $\mu\text{m}$  is of interest. This physical problem can be posed in terms of radiative transfer theory as follows.

Consider a horizontally homogeneous atmosphere, of finite optical depth  $\tau_a$ , illuminated spatially uniformly on top ( $\tau = 0$ ) by monodirectional solar radiation of intensity  $I_0$  incident along  $\Omega_0$  ( $\mu_0 < 0$ ), and bounded at the bottom ( $\tau = \tau_a$ ) by a horizontally heterogeneous vegetation canopy. In the absence of polarization, frequency

shifting interactions and emission, all of which we assume throughout this presentation, the steady state monochromatic radiance or intensity distribution function  $I(\tau, \vec{p}, \Omega)$  is given by

$$(\Omega \cdot \vec{\nabla}_\tau + 1)I(\tau, \vec{p}, \Omega) = \frac{\omega_a}{4\pi} \int_{4\pi} d\Omega' P_a(\Omega' \rightarrow \Omega) I(\tau, \vec{p}, \Omega'), \quad (1a)$$

$$I(0, \Omega) = I_0 \delta(\Omega - \Omega_0), \quad \mu < 0, \quad (1b)$$

$$I(\tau_a, \vec{p}, \Omega) = \frac{1}{\pi} \int_{2\pi} d\Omega' R_v(\vec{p}, \Omega' \rightarrow \Omega) |\mu'| I(\tau_a, \vec{p}, \Omega'), \quad \mu' < 0, \quad \mu > 0. \quad (1c)$$

Here  $\omega_a$  is the single scattering albedo,  $P_a$  is the scattering phase function for photon scattering from the direction  $\Omega'$  into  $\Omega$ , and  $R_v$  is the vegetation canopy directional reflectance factor (BRF). The unit vector  $\Omega(\mu, \varphi)$  has an azimuthal angle  $\varphi$  measured anticlockwise from the positive  $x$ -axis that is directed north, and a polar angle  $\theta = \cos^{-1} \mu$  with respect to the outward normal (opposite to the  $\tau$ -axis, which is directed down into the atmosphere). The operator  $(\Omega \cdot \vec{\nabla}_\tau)$  denotes directional derivative along  $\Omega$  in  $(\tau, \vec{p})$  space, where  $\vec{p} \sim x, y$ .

The canopy bidirectional reflectance factor  $R_v$  that appears in Eq. (1c) can be defined as

$$R_v(\vec{p}, \Omega' \rightarrow \Omega) = \frac{\pi I(\tau_a, \vec{p}, \Omega)}{|\mu'| I(\tau_a, \Omega')}, \quad \mu' < 0, \quad \mu > 0, \quad (2)$$

where  $I(\tau_a, \Omega')$  is the intensity incident on the canopy along  $\Omega'$  and  $I(\tau_a, \vec{p}, \Omega)$  is the surface radiance along  $\Omega$ . The latter is obtained from a numerical solution of the three-dimensional boundary value problem describing radiative transfer in a horizontally heterogeneous vegetation canopy of physical depth  $Z_c$  bounded by a flat anisotropically reflecting soil surface. Specifically,

$$[\Omega \cdot \vec{\nabla} + \sigma(\vec{r}, \Omega)]I(\vec{r}, \Omega) = \int_{4\pi} d\Omega' \sigma_s(\vec{r}, \Omega' \rightarrow \Omega) I(\vec{r}, \Omega'), \quad (3a)$$

$$I(0, \Omega) = \frac{1}{|\mu| \pi} \delta(\Omega - \Omega_0), \quad \mu < 0, \quad (3b)$$

$$I(Z_c, \vec{p}, \Omega) = \frac{1}{\pi} \int_{2\pi} d\Omega' R_s(\vec{p}, \Omega' \rightarrow \Omega) |\mu'| I(Z_c, \vec{p}, \Omega'), \quad \mu' < 0, \quad \mu > 0. \quad (3c)$$

The above assumes spatially uniform incidence of unit flux at the top of the canopy ( $z = 0$ ) and that  $R_s$  is the soil bidirectional reflectance distribution function. A solution of the transport problems defined by Eqs. (1) and (3) simulates top of the atmosphere (TOA) radiance field.

The canopy radiative transfer problem differs from Eq. (3) in that both direct (uncollided) sunlight and diffuse (collided) skylight are incident on the canopy. The atmospheric radiative transfer problem [Eq. (1)] must be solved first in order to properly specify the boundary conditions for the canopy problem. The gov-

Table 1. Atmospheric Parameters Used in the Base Case<sup>a</sup>

Atmospheric Parameters					
Wavelength ( $\mu\text{m}$ )	Incident Energy ( $\text{W/m}^2$ )	Rayleigh Optical Depth	Aerosol Optical Depth	Aerosol Single Scattering Albedo	Anisotropic Parameter
0.4011–0.5133	214.48	0.200	0.282	0.899	0.642
0.5153–0.5333	37.00	0.114	0.242	0.896	0.638
0.5353–0.5873	102.15	0.086	0.225	0.892	0.637
0.5893–0.6852	163.57	0.051	0.194	0.887	0.633
0.6912–0.6972	14.49	0.036	0.175	0.880	0.631
0.8280–0.8940	69.62	0.015	0.132	0.842	0.632

<sup>a</sup> Within these wavelength bands atmospheric absorption is less than 10%. Clear and turbid atmospheric conditions were simulated by doubling and halving the total atmospheric optical depth in each waveband.

erning radiative transfer equation and boundary conditions are

$$[\mathbf{N} \cdot \nabla + \sigma(\tilde{\mathbf{r}}, \mathbf{N})]I(\tilde{\mathbf{r}}, \mathbf{N}) = \int_{4\pi} d\mathbf{N}' \sigma_s(\tilde{\mathbf{r}}, \mathbf{N}' \rightarrow \mathbf{N}) I(\tilde{\mathbf{r}}, \mathbf{N}'), \quad (4a)$$

$$I(0, \tilde{\mathbf{p}}, \mathbf{N}) = I_e \exp\left(-\frac{\tau_a}{|\mu|}\right) \delta(\mathbf{N} - \mathbf{N}_0) + I_d(0, \tilde{\mathbf{p}}, \mathbf{N}), \quad \mu < 0, \quad (4b)$$

$$I(Z_c, \tilde{\mathbf{p}}, \mathbf{N}) = \frac{1}{\pi} \int_{2\pi} d\mathbf{N}' R_s(\tilde{\mathbf{p}}, \mathbf{N}' \rightarrow \mathbf{N}) |\mu'| I(Z_c, \tilde{\mathbf{p}}, \mathbf{N}'), \quad \mu' < 0, \quad \mu > 0, \quad (4c)$$

where  $I_e$  is the extraterrestrial solar radiation incident at the top of the atmosphere along  $\mathbf{N}_0$  about wavelength  $\lambda$  and  $I_d(0, \tilde{\mathbf{p}}, \mathbf{N})$  is the atmospheric intensity distribution incident on the canopy obtained from a numerical solution of the transfer problem denoted by Eq. (5), that is, the atmospheric transmittance. The atmospheric transmittance can be spatially averaged without loss of much accuracy. Further details on problem formulation and algebraic manipulation can be found in Myneni et al. (1990) and in Myneni and Asrar (1993).

## NUMERICAL CONSIDERATIONS

### Atmospheric Parameters

Atmospheric optical depth  $\tau_a$ , single scattering albedo  $\omega_a$ , and phase function  $P_a$  were parameterized for horizontally homogeneous and cloudless atmospheres over midlatitude continental areas. Molecular optical depth  $\tau_m^a$  at wavelength  $\lambda$  was evaluated from refractive index of air and molecular density distribution. Routines from the 5S code were used to calculate  $\tau_m^a$  and the Rayleigh phase function  $P^m$  (Tanré et al., 1990). The profile of atmospheric aerosol distribution was based on a recommendation by the International Radiation Commission (IRC) applicable to continental areas with an aerosol optical depth of 0.23 at 0.55  $\mu\text{m}$  (Deepak and Gerber, 1983). The aerosol scattering phase function  $P^a$  was modeled using the Henyey–Greenstein function. Its asym-

metry parameter  $g^a$  and the aerosol single scattering albedo  $\omega^a$  were tabulated in the IRC report for several wavelengths in the solar spectrum. The total atmospheric optical depth  $\tau_a$ , single scattering albedo  $\omega_a$ , and the scattering phase function  $P_a$  were evaluated assuming external mixing, that is,

$$\tau_a = \tau^m + \tau^a, \quad \omega_a = \frac{\tau^m}{\tau_a} + \omega^a \frac{\tau^a}{\tau_a}, \quad (5a)$$

$$P_a = P^m \frac{\tau^m}{\tau_a} + P^a \frac{\tau^a}{\tau_a}. \quad (5b)$$

A modified version of Lowtran-7 was used to select wavelength bands of atmospheric absorption less than 0.1.<sup>1</sup> Both line and continuum absorption by 16 gaseous species at a solar zenith angle of 30° were considered for selecting these bands. The atmospheric parameters were then integrated over these wavebands assuming a uniform response function (Table 1).

### Canopy Parameters

A horizontally heterogeneous canopy can be simulated as clumps of leaves randomly distributed on a reflective soil with a ground vegetation cover (ground cover, for short) of less than 100%. A flat horizontal ground area ( $a_s$ ) of dimensions 60 m  $\times$  50 m was considered in this study. The height of each shrub (clump)  $Z_c$  was 1 m, with a basal area ( $a_c$ ) of 1 m<sup>2</sup>. Assuming that the clumps do not overlap,  $N_c = (a_s g_c) / a_c$ , where  $g_c$  and  $N_c$  are ground cover and number of clumps in the stand. Nine ground covers ( $g_c = 0.1, 0.2, \dots, 0.9$ ) and two values of clump leaf area index ( $L_c = 1, 5$ ) were considered. In addition, 10 horizontally homogeneous canopies ( $g_c = 1$ ) of  $L_c = 0.25, 0.5, 0.75, 1.0, 1.5, 2.0, 2.5, 3.0, 5.0, 8.0$  were also included for a total of 28 model canopies. The canopy leaf area index  $L$  is, by definition, the product  $L_c \times g_c$ . Thus, the model canopies span the leaf area index range 0.25–8.

<sup>1</sup> S. C. Tsay, personal communication.

Table 2. Canopy and Soil Parameters Used in the Base Case<sup>a</sup>

Canopy and Soil Parameters					
Wavelength ( $\mu\text{m}$ )	Leaf Hemispherical Reflectance	Leaf Hemispherical Transmittance	Single Scattering Albedo of Soil Particulates		
			Sand	Clay	Peat
0.4011–0.5133	0.058	0.008	0.470	0.217	0.061
0.5153–0.5333	0.108	0.061	0.445	0.198	0.045
0.5353–0.5873	0.131	0.084	0.536	0.214	0.054
0.5893–0.6852	0.083	0.038	0.600	0.267	0.074
0.6912–0.6972	0.091	0.051	0.612	0.271	0.081
0.8280–0.8940	0.510	0.418	0.710	0.316	0.194

<sup>a</sup> The leaf optical properties are average values of several measured spectra (F. G. Hall, personal communication). The soil values are taken from Jacquemoud et al. (1992).

A numerical evaluation of the coefficients  $\sigma$  and  $\sigma_s$  in Eqs. (3a) and (4a) requires information on the leaf area density distribution in the stand  $u_L$ , leaf normal orientation distribution  $g_L$ , and the leaf scattering phase function  $\gamma_L$ . Leaf area inside a clump was assumed to be uniformly distributed; thus,  $u_L = L_c / Z_c$ . The leaf normal orientation was assumed azimuthally symmetric and distributed along the polar angle according to planophile, erectophile, and uniform models. Leaf scattering was modeled by the bi-Lambertian (Shultis and Myneni, 1988) and specular reflection functions (Vanderbilt and Grant, 1985), parameterized by measured leaf hemispherical reflectance  $r_L$  and transmittance  $t_L$  (cf. Hall et al., 1992a,b; Table 2).

A quantitative description of the hot spot effect requires consideration of leaf spatial distribution and size in the transport formulation leading to correlated probabilities of photon interactions (Myneni et al., 1991). The resulting equation set is difficult to parameterize and tedious to evaluate. For remote sensing purposes, a simple model of the hot spot effect generally suffices. A model for the extinction coefficient that correlates interaction rates between incident and once-scattered photons is used to describe the hot spot effect in our calculations (Marshak, 1989).

### Soil Parameters

Bidirectional reflectance from the soil surface  $R_s$  was modeled according to Hapke's formulation. The soil was assumed to be a half-space, and first collision intensity was evaluated analytically, including shadows to model the hot spot effect. Multiple scattering was simplified to a two-stream problem. Hapke's model was successfully applied to bare soil surfaces by Jacquemoud et al. (1992). Standard values for the four coefficients ( $b, c, b', c'$ ) of the Legendre polynomial expansion for the particle phase function, and the parameter  $h$  related to the porosity of the medium are given in Jacquemoud et al. (1992). The only parameter dependent on wavelength and soil moisture is the single scattering albedo of the soil particulates  $\omega_s$ . These were obtained by digitizing their Figure

4 ( $\omega_s$  vs. wavelength) for three soil particulate types—clay, sand, and peat. These were then integrated over the wavebands of interest and used to parameterize the soil BRDF model (Table 2).

### Numerical Solution

The radiative transfer problems denoted by Eqs. (1), (3), and (4) were numerically solved by the discrete ordinates method in three spatial dimensions (Myneni et al., 1990). The angular variable  $\Omega$  was discretized using  $EQ_N$  quadrature sets. The spatial derivatives were approximated by first-order finite-difference schemes. The resulting algebraic system of equations was solved iteratively on the distributed source by the method of sweeping in the phase-space grid. A coarse-mesh rebalancing method for accelerating this iteration was implemented together with methods to alleviate numerical maladies such as negative intensities, oscillatory distortions, ray effects, etc. A  $30 \times 30 \times 10$  spatial grid and an  $EQ_6$  quadrature (48 directions in the unit sphere) were used unless specified otherwise.

The calculation scheme is as follows; details are given in Myneni and Asrar (1993). The canopy BRF matrix  $R_v$  is evaluated first by numerically solving the boundary value problem denoted by Eq. (3). The atmospheric transfer problem [Eq. (1)] is then solved using this matrix. The radiation field incident on the canopy is now known. Thus, the canopy transfer problem [Eq. (5)] can be numerically evaluated. A detailed energy balance is performed at each level. We also implemented interpolation schemes to decouple quadrature orders between the canopy and atmospheric radiative transfer calculations. Essentially this involves performing one additional sweep of the spatial grid, using converged source distribution, into the desired angular grid. The entire scheme is wavelength specific requiring about 80 Sparcstation-2 CPU min.

### Base Case and Sensitivity Analysis

A base case was defined in terms of parameter values considered typical from a remote sensing point of view.

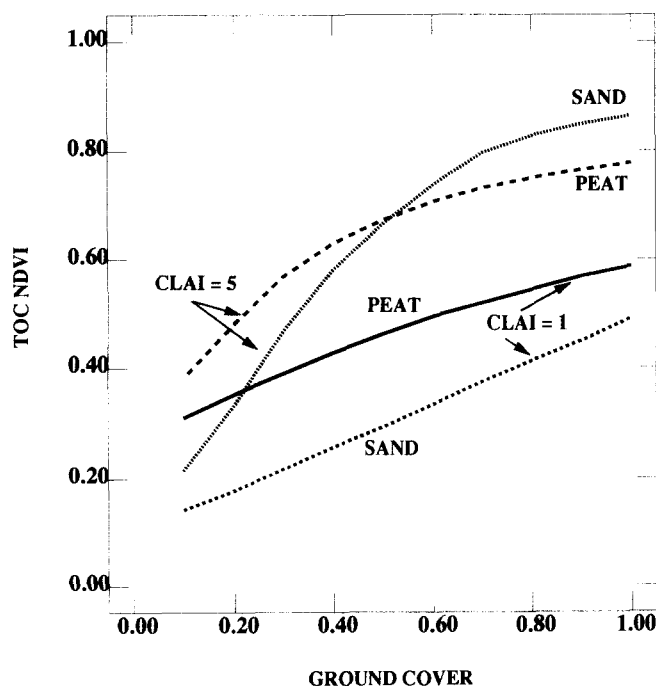


Figure 1. Relationship between top of the canopy (TOC) NDVI vs. ground cover for two values of clump leaf area indices (CLAI) and soils. The other problem parameters are as in the base case.

The base case consisted of the 28 model canopies discussed above with a uniform leaf angle and leaf area density distribution. The index of refraction for leaf cuticular surface we used was 1.5, and assumed to be wavelength-independent. A standard value of 4.0 for the hot spot parameter (ratio of clump height to characteristic leaf dimension) was used throughout (Stewart, 1990). Leaf hemispherical reflectance and transmittance were averages of measured values for green leaves (Table 2). A clayey soil was assumed for the base case together with a standard cloudless atmosphere to simulate the boundary conditions (Tables 1 and 2). Finally, the solar zenith and azimuth angles in the base case were  $30^\circ$  and  $225^\circ$ .

A sensitivity analysis was performed by changing the base case parameter values one at a time. Sensitivity to leaf orientation was investigated by changing the uniform distribution to a planophile and an erectophile distribution. Similarly, the leaf optical properties in the PAR wavelengths were varied by  $\pm 20\%$  to simulate bright and dark leaves. Sensitivity to soil reflectance was performed by substituting the clayey soil with sandy and peaty soils. Turbid and clear atmospheric conditions were simulated by doubling and halving the aerosol optical depths used in the base case (Table 1). Finally, sensitivity to solar angle was studied by changing it from  $30^\circ$  in the base case to  $5^\circ$  and  $60^\circ$ .

## RESULTS AND DISCUSSION

### Dynamics of NDVI

The relationship between top of the canopy normalized difference vegetation index (TOC NDVI) and ground cover (GC) for heterogeneous canopies with varying clump leaf area index (CLAI of 1 and 5) and soil reflectance (sand and peat) is shown in Figure 1. TOC NDVI increases with ground cover, the slope of which depends on clump leaf area index and soil reflectance. This relationship is generally linear for canopies of sparse clumps (CLAI = 1). At a given ground cover, canopies with dense clumps (CLAI = 5) have a higher TOC NDVI than those with sparse clumps. This does not imply that TOC NDVI is indicative of canopy leaf area index, which by definition is the product of ground cover and clump leaf area index. For instance, at a given canopy leaf area index, say LAI = 1, canopies with sparse clumps and complete ground cover (CLAI = 1 and GC = 1) have a higher TOC NDVI than those with dense clumps and low ground cover (CLAI = 5 and GC = 0.2). Thus, TOC NDVI is responsive to the spatial distribution of leaf area and not simply to the absolute amount of such leaf area. Such an interpretation is more meaningful because the concept of canopy leaf area index can be defined rigorously only in the limiting case of complete ground cover (GC = 1).

The influence of soil reflectance on TOC NDVI can be clearly seen in Figure 1. TOC NDVI, which is a measure of surface reflectance contrast between near-infrared and red wavelengths, is not necessarily high, even though the component spectral reflectances may be high. For instance, with similar ground cover and clump leaf area indices, canopies with a dark soil background (peat) have a higher TOC NDVI than those with a bright soil background (sand). This is generally valid for sparse clumps. With increase in clump leaf area index and ground cover, canopies with a bright background have a higher TOC NDVI than those with a darker background (Fig. 1; CLAI = 5; GC > 0.5). This illustrates the importance of the interaction between pixel heterogeneity and background effects on the interpretation of TOC NDVI.

Pixel heterogeneity can be conceptually quantified on a macroscopic scale by ground cover and clump leaf area index. Structural and optical properties of clumps within a pixel are variable under natural conditions. As a first approximation, we may assume that the clumps in a pixel are identical as far as their leaf area index is concerned. Changes in leaf normal orientation and leaf optical properties (hemispherical reflectance and transmittance) are then, conceptually, the microscopic aspect of pixel heterogeneity. For instance, two pixels identical in ground cover, clump leaf area index, and leaf optical properties but different in leaf normal orientation are likely to have different TOC NDVIs. It is this aspect of

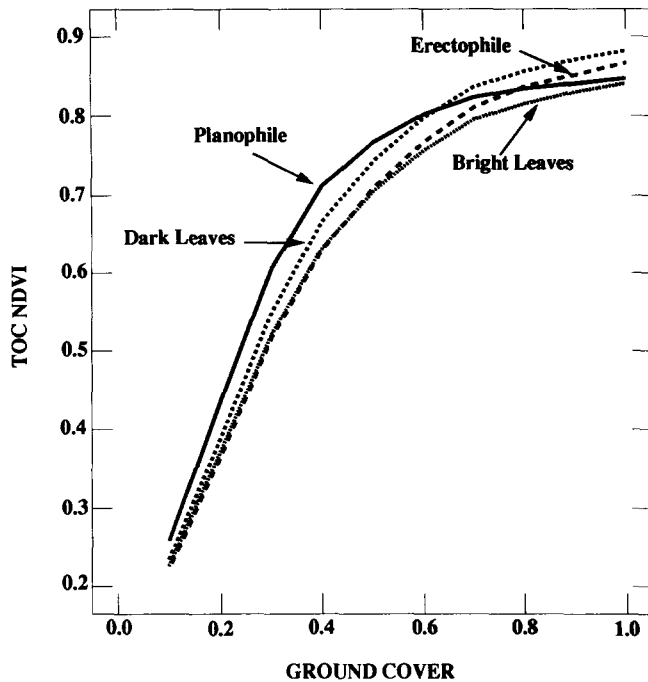


Figure 2. Relationship between top of the canopy (TOC) NDVI vs. ground cover. The other problem parameters are as in the base case.

pixel heterogeneity's impact on NDVI that we consider next.

The relationship between TOC NDVI and ground cover is shown for canopies with planophile (mostly horizontal leaves) and erectophile (mostly vertical leaves) leaf orientations in Figure 2. Canopies with horizontal leaves intercept more of the incident radiation field than those with erect leaves. Consequently, the former tend to have a higher canopy reflectance, especially in the near-infrared where multiple scattering dominates the reflected radiation field. More importantly, leaf orientation influences the angular distribution of the canopy spectral reflectance field (Kimes, 1984). Thus, NDVIs evaluated from off-nadir view directions are likely to differ far more significantly than the nadir values presented in Figure 2.

Leaf or needle optical properties of green vegetation can vary depending upon age, nutritional status, water conditions, light history (sunlit or shaded), pollution, etc. (Williams, 1991). Moreover, a canopy sensed with instruments of different bandwidths but equivalent response functions, centered about the same wavelength, can result in different values of canopy reflectance, depending upon the integral leaf optical property perceived by the instrument within its waveband. In Figure 2, the relationship between TOC NDVI and ground cover for canopies with  $\pm 20\%$  deviations from mean leaf hemispherical reflectance and transmittance at PAR wavelengths is shown. Canopies with bright leaves tend

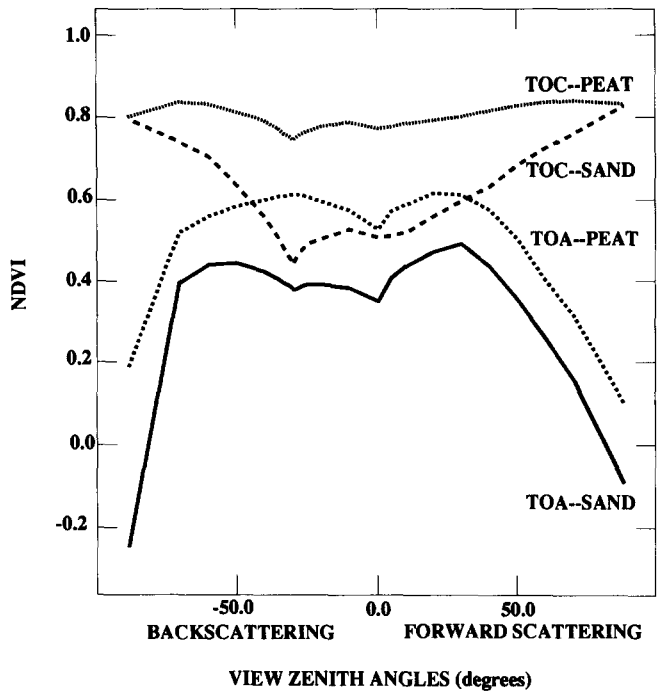


Figure 3. Top of the atmosphere (TOA) and top of the canopy (TOC) NDVI as a function of view zenith angle in the principal plane. The solar zenith angle is  $30^\circ$ , and the other problem parameters are as in the base case.

to have a lower TOC NDVI than those with darker leaves due to a higher canopy reflectance at red, as may be expected. It should be noted that, in these calculations, the sum of leaf reflectance and transmittance was not allowed to exceed unity based on physical arguments.

The angular distribution of canopy bidirectional reflectance is anisotropic and depends on the solar angles and wavelength (Deering, 1989). At wavelengths of strong chlorophyll absorption, viz., blue and red, backscattering is dominant, and the distribution exhibits a characteristic hot spot effect in the retrosolar direction. In the strongly scattering near-infrared region of the spectrum, anisotropy is less prevalent but the distributions are nevertheless not isotropic. A rough soil surface also exhibits the hot spot effect and its reflectance distributions are similarly anisotropic (Jacquemoud et al., 1992). The dependence of soil bidirectional reflectance on wavelength is different than that of vegetation because the interaction mechanisms are different. Hence, the surface bidirectional reflectance distributions in situations of incomplete ground cover are complex combinations of both canopy and soil distributions. If such a scene is repeatedly viewed from different directions, as in the case of the Advanced Very High Resolution Radiometer, surface bidirectional effects are manifest in the temporal distributions of NDVI. This is illustrated in Figure 3 for an incomplete canopy of ground cover 0.3 and clump

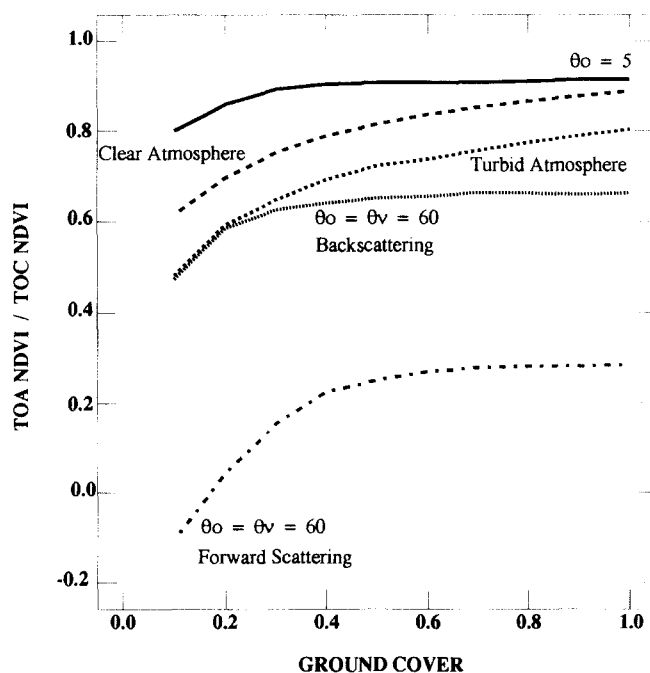


Figure 4. Transmissivity of NDVI vs. ground cover. Here  $\theta_0$  and  $\theta_v$  are the solar and view zenith angles.

leaf area index 5. A dark and a bright background are chosen to illustrate the importance of soil reflectance on both TOC and top of the atmosphere (TOA) NDVIs. The vegetation indices were evaluated from surface bidirectional reflectances in the principal plane, at a solar zenith angle of  $30^\circ$ .

The TOC NDVI distribution in the principal plane has a minimum value about the retrosolar direction because the hot spot effect increases reflectance in the red band. Thus, the reflectance contrast between near-infrared and red is decreased. As seen earlier (Fig. 1), canopies with a dark background have higher TOC NDVIs than those with a brighter background at a ground cover of 0.3 and clump leaf area index of 5. The angular distributions also show a minimum about the nadir direction. TOA NDVI is less than TOC NDVI because of the positive (negative) atmospheric effect at the red (near-infrared) wavelength. The most characteristic feature of the TOA NDVI distribution is its steep decrease at oblique view directions ( $>60^\circ$ ). Path radiance increases with zenith angle and rather steeply at oblique directions. The magnitude of path radiance is higher at short wavelengths, for instance red as opposed to near-infrared, due to molecular and aerosol scattering. Hence, the contrast between near-infrared to red spectral reflectance is greatly reduced along oblique view directions. From Figure 3, it can be seen that sensing about the nadir reduces the bidirectional effects, and off-nadir observations of TOA NDVI must be corrected for both atmospheric and bidirectional effects.

The ratio of top of the atmosphere to top of the canopy vegetation index can be considered as the transmissivity of an index that denotes the extent of atmospheric and bidirectional effects. The influence of atmospheric effects on the transmissivity of NDVI at various ground covers is shown in Figure 4 for two solar zenith angles ( $\theta_0$ ) and atmospheric optical depths ( $\tau_a$ ). Transmissivities along a backscattering and a forward scattering direction in the principal plane for  $\theta_0 = 60^\circ$  are also shown in Figure 4. The transmissivity of NDVI increases with ground cover and decreases with increasing  $\theta_0$  and  $\tau_a$ . For near-nadir sun positions, NDVI transmissivities are generally greater than 0.8. At oblique solar incidences ( $\theta_0 = 60^\circ$ ), the transmissivity of NDVI can vary from 0.2 to 0.5 depending upon the view direction and ground cover. The transmissivity is poorest in the forward scattering directions because of the large atmospheric effect. These results indicate that near-nadir solar incidences and clear atmospheric conditions are most conducive for remote sensing, with transmissivities as high as 0.8 for NDVI. Under these conditions, TOA observations need correction only for the atmospheric effects. Off-nadir observations must be corrected for bidirectional effects as well.

#### Dynamics of FAPAR

The fraction of photosynthetically active radiation absorbed by the photosynthetic tissue in a vegetation canopy (FAPAR) depends on the incident radiation field, architecture and optics of the canopy, and the reflectance of the soil background. The evaluation of FAPAR requires integration of the spectral absorptance over the  $0.4\text{--}0.7\ \mu\text{m}$  wavelength interval (Myneni et al., 1992). From an empirical point of view, the accuracy of FAPAR evaluation depends on the spectral bands of a sensor and the availability of concurrent measurements of incident radiation field. From a theoretical point of view, there are at least five wavebands within the  $0.4\text{--}0.7\ \mu\text{m}$  interval where atmospheric absorption is less than 10% (Tables 1 and 2). On an average, about 90% of PAR is incident in three bands:  $0.401\text{--}0.513\ \mu\text{m}$ ,  $0.535\text{--}0.587\ \mu\text{m}$ , and  $0.589\text{--}0.685\ \mu\text{m}$  (0.38, 0.20, and 0.32, respectively). The contribution of these bands to FAPAR is, on an average, 0.35, 0.19 and 0.36, respectively. That is, FAPAR can be evaluated to 90% of its true value, if these three wavebands are considered. Interestingly, FAPAR can be estimated to 95% of its true value by the waveband  $0.589\text{--}0.685\ \mu\text{m}$ . Thus, the fraction of radiation absorbed by the canopy at red wavelength is a good approximation of the fraction of total PAR absorbed.

The relationship between FAPAR and ground cover is shown in Figure 5 for two clump leaf area indices (CLAI = 1 and 5) and two backgrounds (sand and peat). Canopy absorption increases with clump leaf area index

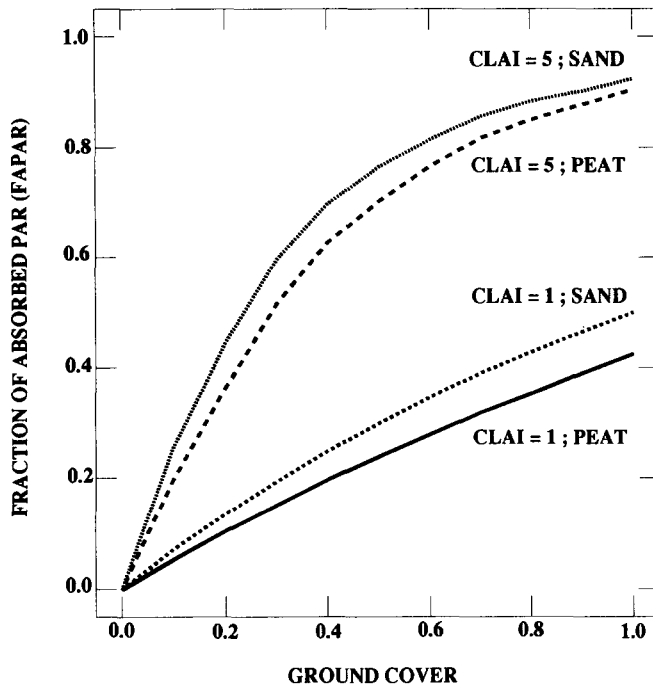


Figure 5. Relationship between the fraction of PAR absorbed by the canopy (FAPAR) vs. ground cover for two values of clump leaf area indices (CLAI) and soils. The other problem parameters are as in the base case.

and soil reflectance. The relationship is linear (nonlinear) for sparse (dense) clumps, irrespective of the background reflectance. From these results, it may be inferred that the relation between LAI and FAPAR is near-linear at LAIs  $< 3$ , after which it tends to an asymptotic value of 0.95 depending on the canopy, soil, and atmospheric parameters.

The influence of leaf normal orientation, atmospheric turbidity and solar zenith angle on the relationship between FAPAR and ground cover is shown in Figure 6. Planophile canopies have a higher PAR absorption than erectophile canopies at moderate solar zenith angles ( $\theta_0 = 30^\circ$ ) because of increased interception of incident radiation field. Radiation absorption is also dependent on the solar zenith angle, with FAPAR increasing for oblique incidences. The relationship between FAPAR and ground cover is generally linear for near-nadir incidences ( $\theta_0 = 5^\circ$ ), and, at nearly complete ground covers, canopy absorption is greater than for  $\theta_0 = 60^\circ$ . Atmospheric optical depth also plays a less dominant role in determining PAR absorption. FAPAR decreases with atmospheric optical depth; that is, radiation absorption under clear atmospheric conditions is higher than under turbid conditions. The fraction of direct sunlight in the radiation field incident on the canopy decreases with atmospheric optical depth, especially more so at shorter wavelengths due to increased molecular scattering (e.g., red compared with near-infrared). Consequently, the

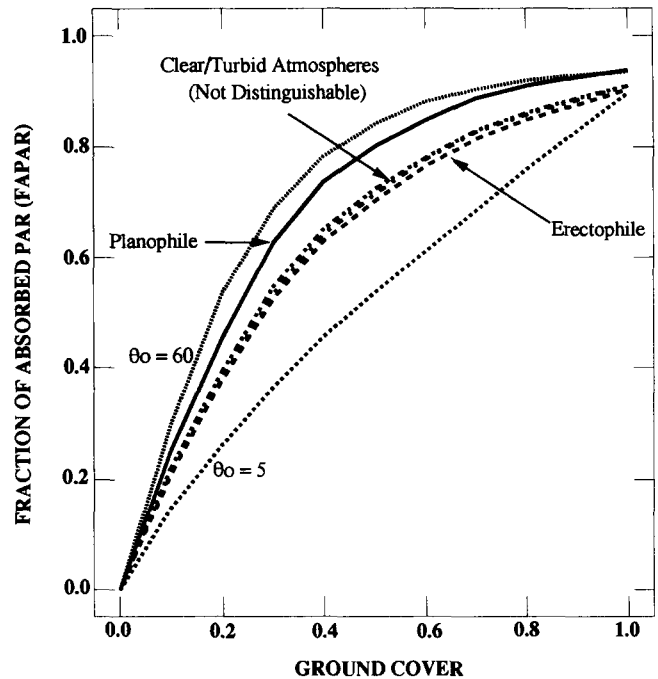


Figure 6. Relationship between the fraction of PAR absorbed by the canopy (FAPAR) vs. ground cover. Here  $\theta_0$  is the solar zenith angle. The other problem parameters are as in the base case.

fraction of PAR absorbed by the canopy decreases as atmospheric turbidity increases.

In conclusion, FAPAR increases with ground cover, clump leaf area index, background reflectance, and solar zenith angle. It decreases with increase in leaf hemispherical reflectance and transmittance (results not shown), mean leaf angle, and atmospheric optical depth. Although FAPAR is functionally related to ground cover and clump leaf area index in a way similar to NDVI, for other parameters (viz., soil reflectance), the response is quite different.

### Relationship between FAPAR and NDVI

We have seen that both NDVI (Fig. 1) and FAPAR (Fig. 5) respond to the amount of leaf area in a vegetation canopy. Therefore, we may expect a causal relationship between FAPAR and NDVI. The nature of this relationship and how it varies with changes in canopy, soil, and atmospheric parameters is the subject of our discussion here.

The relationship between FAPAR and TOC NDVI for planophile and erectophile homogeneous ( $GC = 1$ , varying LAI) and heterogeneous ( $CLAI = 5$ , varying ground cover) canopies is shown in Figure 7. Planophile and erectophile distributions denote extremes of leaf orientation. Yet, the relationship between FAPAR and TOC NDVI is nearly invariant. We have seen that planophile canopies have a higher NDVI (Fig. 2) and

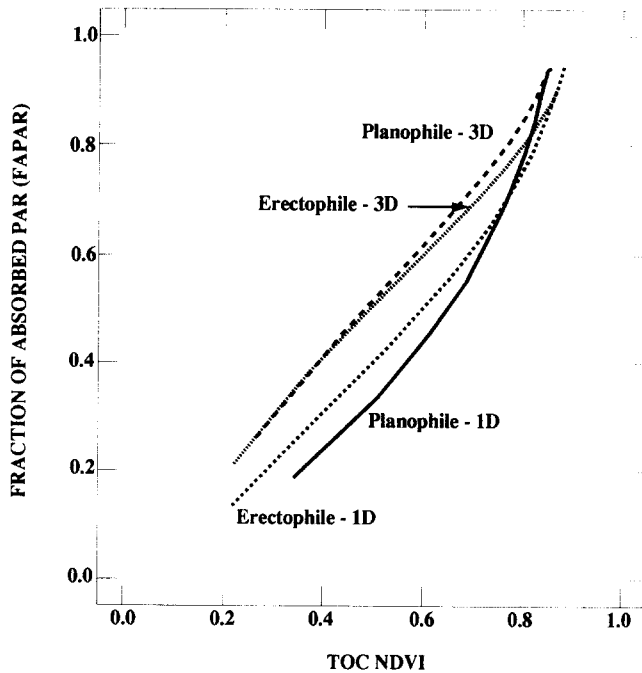


Figure 7. The relationship between FAPAR and top of the canopy (TOC) NDVI in homogeneous (1D) and heterogeneous (3D) canopies with different leaf orientation distributions. The other problem parameters are as in the base case.

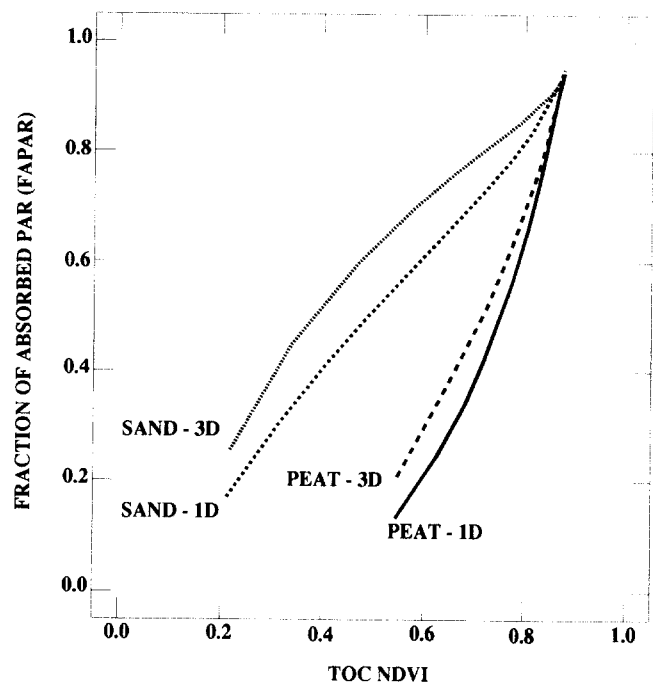


Figure 8. The relationship between FAPAR and top of the canopy (TOC) NDVI in homogeneous (1D) and heterogeneous (3D) canopies with different soil backgrounds. The other problem parameters are as in the base case.

PAR absorption (Fig. 6) than erectophile canopies because of increased projected area to the incident radiation field. Therefore, it appears that both FAPAR and NDVI are similarly influenced by leaf orientation which explains the invariance of this relationship. Similar results (not shown here) were obtained for  $\pm 20\%$  variations in leaf optical properties.

It can also be seen from Figure 7 that the relationship between FAPAR and TOC NDVI is nearly similar for homogeneous (1D) and heterogeneous (3D) canopies. This important result indicates that the relationship is independent of pixel heterogeneity. There is a near-unique correspondence between TOC NDVI and FAPAR regardless of the spatial distribution of leaf area in a pixel. A given value of TOC NDVI can result from various configurations of ground cover and clump leaf area index. In all such cases, FAPAR is nearly unique. One may also interpret this relationship to be scale-invariant, that is, pixels of different spatial scales but of the same TOC NDVI are likely to have the same FAPAR values.

The above result does not contradict our earlier observation that TOC NDVI is responsive to pixel heterogeneity. Indeed, if pixels of different clump leaf area indices and/or ground covers result in different values of TOC NDVI, then the corresponding FAPAR values will be different. For instance, at a ground cover of 0.5, TOC NDVI is 0.46 and FAPAR = 0.25 if CLAI = 1, and TOC NDVI = 0.67 and FAPAR = 0.70 if CLAI = 5 (Fig.

1). However, a TOC NDVI of 0.5 can be realized for two canopies of GC = 0.7, CLAI = 1, and GC = 0.22, CLAI = 5. In both instances, the value of FAPAR is approximately 0.35–0.38 (Fig. 5). It is this fact that leads us to conclude that the relationship between FAPAR and TOC NDVI is independent of pixel heterogeneity, and thus, is scale invariant.

Background reflectance influences TOC NDVI and FAPAR differently. An increase in soil reflectance decreases TOC NDVI (Fig. 1) and increases FAPAR (Fig. 5). Thus, the relationship between TOC NDVI and FAPAR is significantly affected by soil reflectance (Fig. 8). The relationship is increasingly linear with background reflectance. However, it is nearly similar for homogeneous (1D) and heterogeneous canopies (3D), irrespective of the soil reflectance. Nevertheless, the results indicate that if TOC NDVI measurements were to serve as diagnostics of FAPAR, soil reflectance must be known with some accuracy or alternate methods to minimize background contribution to the remote measurement should be devised (Huete, 1988).

The influence of solar zenith angle on the relationship between FAPAR and NDVI is shown in Figure 9. TOA NDVI is less than TOC NDVI because of the positive atmospheric effect at red and negative atmospheric effect at the near-infrared wavelength. The shift in the relationship between FAPAR and NDVI, when TOA radiances are used instead of TOC radiances,

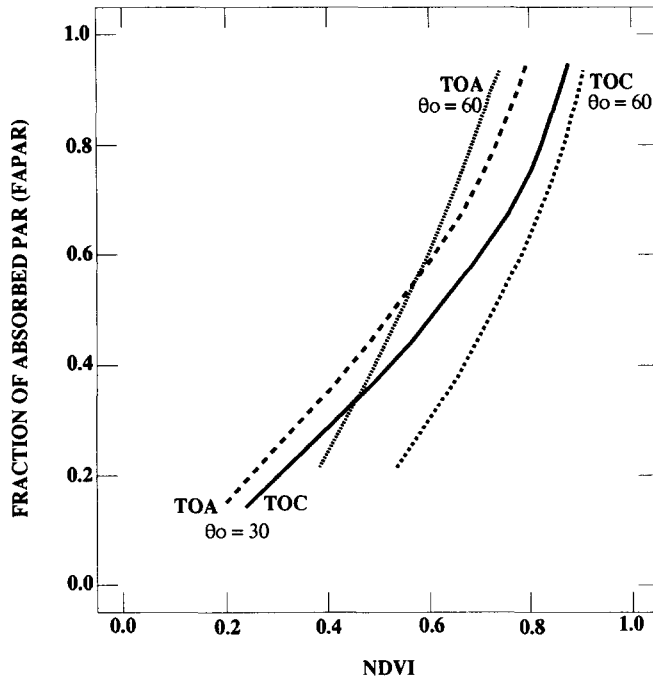


Figure 9. The relationship between FAPAR and NDVI in homogeneous canopies at different solar zenith angles  $\theta_0$ . Both top of the atmosphere (TOA) and top of the canopy (TOC) NDVIs are shown. The other problem parameters are as in the base case.

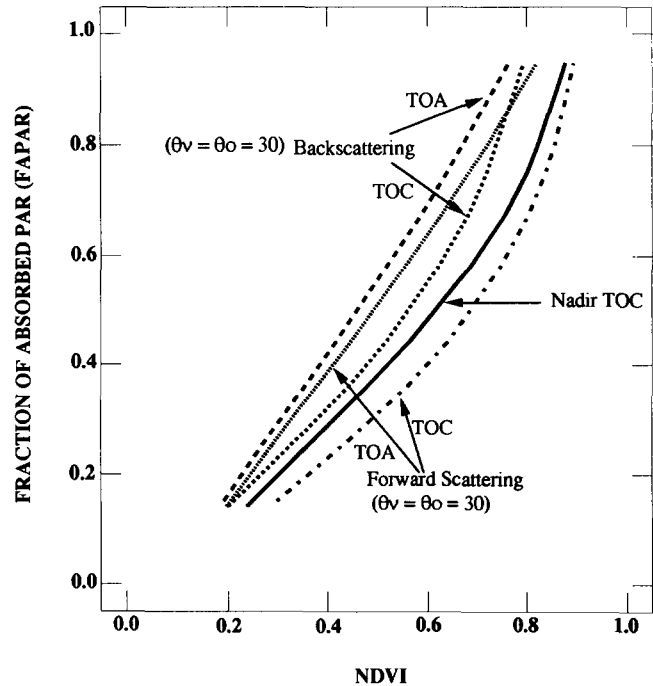


Figure 10. The relationship between FAPAR and NDVI in homogeneous canopies for a solar zenith angle of  $30^\circ$ . Both top of the atmosphere (TOA) and top of the canopy (TOC) NDVIs are shown. Here  $\theta_v$  is the view zenith angle. The other problem parameters are as in the base case.

indicates the magnitude of atmospheric effects. The intercept of the relationship between FAPAR and TOC NDVI is generally negative, indicating bare soil NDVI when FAPAR is zero. However, the intercept of the relationship between FAPAR and TOA NDVI can be positive because of atmospheric effects.

Radiation absorption by the canopy and TOC NDVI both increase with solar zenith angle due to increased interception of the incident radiation field. The slope of the relationship between FAPAR and TOC NDVI remains invariant, while the  $x$ -axis intercept (bare soil NDVI) increases with increasing solar zenith angle. Atmospheric effects increase with solar zenith angle; thus, the transmissivity of NDVI decreases substantially. As a result, the  $y$ -axis intercept of FAPAR and TOA NDVI relationship increases with solar zenith angle. Similar results are obtained when atmospheric optical depth is increased which decreases the transmissivity of NDVI (Fig. 4). These results clearly indicate a need for correcting the atmospheric effects.

Bidirectional effects due to surface reflectance anisotropy play a large role in the remote sensing of FAPAR, in addition to atmospheric effects, when off-nadir observations of NDVI are used. This is illustrated in Figure 10, where off-nadir relationships between TOA and TOC NDVIs in the forward and backscattering directions with FAPAR are presented. With increase in leaf area, off-nadir canopy reflectance at near-infrared

increases while red reflectance decreases. As a result, TOC NDVI increases with view zenith angle in the principal plane, except for the minimum encountered about the retrosolar direction due to the hot spot effect which increases red reflectance substantially (Fig. 3). Moreover, canopy reflectance in oblique view directions saturates at a lower value of canopy leaf area than in near-nadir directions. Thus, the relationship between FAPAR and off-nadir TOC NDVI is nonlinear, reaching an asymptotic value at NDVIs of 0.8–0.9, depending on the view zenith angle. At equivalent view zenith angles, TOC NDVIs in the forward scattering directions are higher than those in the backscattering directions because of reduced canopy reflectance at red. The relationship with FAPAR is similarly affected.

In addition to surface bidirectional effects, the angular distribution of atmospheric effects impacts the relationship between FAPAR and TOA NDVI. Atmospheric path radiance increases with view zenith angle, and rather steeply in oblique directions. Forward scattering is dominant in the atmosphere compared to backscattering. As a result, transmissivity of NDVI decreases with view zenith angle and is much lower for forward scattering than backscattering (Fig. 4). The relationship between FAPAR and TOA NDVI reflects these surface and atmospheric bidirectional effects if such NDVIs are evaluated from off-nadir TOA radiances in the forward and backscattering directions (Fig. 10). These relation-

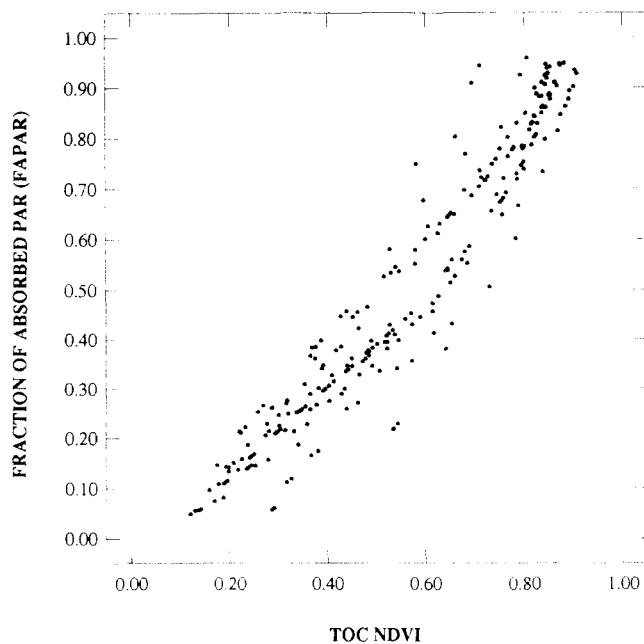


Figure 11. The relationship between FAPAR and top of the canopy (TOC) NDVI. Results from bright (sand) and dark (peat) soil sensitivity cases are not included in this plot. A linear model fits the data very significantly ( $r^2 = 0.919$ ,  $N = 252$ ). The slope of the relationship is 1.1638 with an intercept of  $-0.1426$ . Thus, the linear model gives a bare soil NDVI of 0.1225 (when FAPAR = 0.0). This linear model or algorithm for FAPAR is valid for: a) solar zenith angle less than  $60^\circ$ ; b) view zenith angles about the nadir; c) soils or backgrounds of moderate brightness (NDVI about 0.12); d) atmospheric optical depths less than 0.65 to 550 nm.

ships are increasingly nonlinear with view zenith angle. They are not unique functions of view zenith angle because of angular differences in forward and backscattering.

#### An Algorithm for Estimating FAPAR

There are sufficient causal grounds for relating FAPAR to NDVI. The relationship is independent of pixel heterogeneity, parameterized here with ground cover, clump leaf area index, and variations in leaf orientation and optical properties. On the other hand, it is sensitive to background, atmospheric, and bidirectional effects. A simple model or an algorithm for estimating FAPAR from NDVI can still be derived.

Atmospheric and bidirectional effects may be ignored if we restrict our analysis to nadir TOC NDVI. Further, if we consider backgrounds of moderate brightness, background effects may also be ignored. The resulting relationship between FAPAR and nadir TOC NDVI is shown in Figure 11. A linear model fits the data very significantly ( $r^2 = 0.919$ ,  $N = 252$ ). The slope of the relationship is 1.164 with an intercept of  $-0.143$ . Thus, the linear model gives a bare soil NDVI of 0.123 (when FAPAR = 0.0). This relationship compares well

with empirical relations reported in the literature (Asrar et al., 1984; Wiegand et al., 1992; Hall et al., 1992a,b; among others).

This linear model or algorithm for FAPAR is valid for: a) solar zenith angle less than  $60^\circ$ ; b) view zenith angles about the nadir or less than  $30^\circ$ ; c) soils or backgrounds of moderate brightness (NDVI about 0.12); d) atmospheric optical depths less than 0.65 at 550 nm.

This simplified model of the relationship between FAPAR and TOC NDVI must be seen as a typical or an average model, for it is derived to represent a large canopy problem parameter space (ground cover, leaf area, leaf orientation, and optical properties). For this very reason, it may poorly represent the relationship between FAPAR and TOC NDVI in a particular situation. Moreover, the limitations of the radiative transfer model must be recognized. For instance, stems, branches, and other woody components are not included in the model. The concept of pixel heterogeneity proposed here is dictated by the nature of our model and represents the least complex of possible scenarios. A pixel under natural conditions may consist of different plant species (needle and leaf canopies) with a complex structure (crown and understory vegetation). A model that can accommodate realism to such a degree is bound to be far more complicated and is beyond the current state-of-the-art. In spite of these caveats, it is hoped that the algorithm presented here has some practical applications.

#### CONCLUDING REMARK

A linear, scale invariant relationship exists between the fraction of photosynthetically active radiation absorbed by the photosynthesizing tissue in a vegetation canopy (FAPAR) and top of the canopy normalized difference vegetation index (TOC NDVI). However, when using satellite data, atmospheric and bidirectional effects must be corrected, and background contributions to the signal must be accounted for.

*This work was made possible with the financial support of NASA Grant NAS5-30442. We thank Dr. S. C. Tsay for providing us with a modified version of the LOWTRAN-7 code to evaluate atmospheric absorption.*

#### REFERENCES

- Asrar, G., Fuchs, M., Kanemasu, E. T., and Hatfield, J. H. (1984), Estimating absorbed photosynthetic radiation and leaf area index from spectral reflectance in wheat, *Agron. J.* 76:300-306.
- Asrar, G., Myneni, R. B., and Choudhury, B. J. (1992), Spatial heterogeneity in vegetation canopies and remote sensing of absorbed photosynthetically active radiation: a modeling study, *Remote Sens. Environ.* 41:85-103.

- Baret, F., and Guyot, G. (1991), Potential and limits of vegetation indices for LAI and APAR assessment, *Remote Sens. Environ.* 35:161–173.
- Choudhury, B. J. (1987), Relationships between vegetation indices, radiation absorption, and net photosynthesis evaluated by a sensitivity analysis, *Remote Sens. Environ.* 22: 209–233.
- Daughtry, C. S. T., Gallo, K. P., and Bauer, M. E. (1983), Spectral estimates of solar radiation intercepted by corn canopies, *Agron. J.* 75:527–531.
- Deepak, A., and Gerber, H. E. (Eds.) (1983), *Report of WMO (CAS)/Radiation Commission of IAMAP Meeting of Experts on Aerosols and Their Climatic Effects, (Williamsburg, Virginia, USA, 28–30 March, 1983), Report No. WCP-55, World Meteorological Organisation, Geneva.*
- Deering, D. W. (1989), Field measurements of bidirectional reflectance, in *Theory and Applications of Optical Remote Sensing* (G. Asrar, Ed.), Wiley, New York, pp. 14–61.
- Gallo, K. P., Daughtry, C. S. T., and Bauer, M. E. (1985), Spectral estimation of absorbed photosynthetically active radiation in corn canopies, *Remote Sens. Environ.* 17:221–232.
- Goward, S. N., and Huemmrich, K. F. (1992), Vegetation canopy PAR absorptance and the normalized difference vegetation index: An assessment using the SAIL model, *Remote Sens. Environ.* 39:119–140.
- Hall, F. G., Huemmrich, K. F., Goetz, S. J., Sellers, P. J., and Nickerson, J. E. (1992a), Satellite remote sensing of surface energy balance: success, failures, and unresolved issues in FIFE, *J. Geophys. Res.* 97:19,061–19,089.
- Hall, F. G., Huemmrich, K. F., Strebel, D. E., Goetz, S. J., Nickerson, J. E., and Woods, K. D. (1992b), Biophysical, morphological, canopy optical property, and productivity data from the Superior National Forest, NASA Technical Memorandum 104568, Washington, DC.
- Hatfield, J. L., Asrar, G., and Kanemasu, E. T. (1984), Intercepted photosynthetically active radiation estimated by spectral reflectance, *Remote Sens. Environ.* 14:65–75.
- Huete, A. R. (1988), A soil-adjusted vegetation index (SAVI), *Remote Sens. Environ.* 25:295–309.
- Jacquemoud, S., Baret, F., and Hanocq, J. F. (1992), Modeling spectral and bidirectional soil reflectance, *Remote Sens. Environ.* 41:123–132.
- Kaufman, Y. J. (1989), The atmospheric effect on remote sensing and its corrections, in *Theory and Applications of Optical Remote Sensing* (G. Asrar, Ed.), Wiley, New York, pp. 336–428.
- Kimes, D. S. (1984), Modeling the directional reflectance from complete homogeneous vegetation canopies with various leaf-orientation distributions, *J. Opt. Soc. Am.* 1:725–737.
- Marshak, A. L. (1989), The effect of the hot spot on the transport equation in plant canopies, *J. Quant. Spectrosc. Radiat. Transfer* 42:615–630.
- Myneni, R. B., and Asrar, G. (1993), Radiative transfer in three dimensional atmosphere vegetation media, *J. Quant. Spectrosc. Radiat. Transfer* 49:585–598.
- Myneni, R. B., Asrar, G., and Gerstl, S. A. W. (1990), Radiative transfer in three dimensional leaf canopies, *Trans. Theory Stat. Phys.* 19:205–250.
- Myneni, R. B., Marshak, A. L., and Knyazikhin, Yu. (1991), Transport theory for leaf canopies with finite dimensional scattering centers, *J. Quant. Spectrosc. Radiat. Transfer* 46: 259–280.
- Myneni, R. B., Asrar, G., Tanré, D., and Choudhury, B. J. (1992), Remote sensing of solar radiation absorbed and reflected by vegetated land surfaces, *IEEE Trans. Geosci. Remote Sens.* GE-30:302–314.
- Prince, S. D. (1991), A model of regional primary production for use with coarse resolution satellite data, *Int. J. Remote Sens.* 12:1313–1330.
- Sellers, P. (1985), Canopy reflectance, photosynthesis and transpiration, *Int. J. Remote Sens.* 8:1335–1372.
- Shultis, J. K., and Myneni R. B. (1988), Radiative transfer in vegetation canopies with anisotropic scattering, *J. Quant. Spectrosc. Radiat. Transfer.* 39:115–129.
- Stewart, R. (1990), Modeling radiant energy transfer in vegetation canopies, M.S. thesis, Kansas State University, Manhattan.
- Tanré, D., Deroo, C., Duhaut, P., et al. (1990), Description of a computer code to simulate the satellite signal in the solar spectrum: the 5S code, *Int. J. Remote Sens.* 11:659–668.
- Tucker, C. J. (1979), Red and photographic infrared linear combinations for monitoring vegetation, *Remote Sens. Environ.* 8:127–150.
- Vanderbilt, V. C., and Grant, L. (1985), Plant canopy specular reflectance model, *IEEE Trans. Geosci. Remote Sens.* GE-23:722–730.
- Wiegand, C. L., Richardson, A. J., Escobar, D. E., and Gerbermann, A. H. (1991), Vegetation indices in crop assessments, *Remote Sens. Environ.* 35:105–119.
- Wiegand, C. L., Maas, S. J., Aase, J. K., et al. (1992), Multispectral analyses of spectral-biophysical data for wheat, *Remote Sens. Environ.* 42:1–21.
- Williams, D. L. (1991), A comparison of spectral reflectance properties at the needle, branch, and canopy level for selected conifer species, *Remote Sens. Environ.* 35:79–93.